

Effect of Branch Angle and Magnetic Field on the Flow through a Bifurcating Vessel: Application to Arterial Blood Flow

M. K. Sharma¹, Kuldip Singh², Seema Bansal³

^{1,2,3} Department of Mathematics, Guru Jambheshwar University of Science & Technology, Hisar-125001(Haryana)

Abstract: Flow pattern depends highly on the local geometry such as branching and sites of stenosis. In circulatory system, the periodic nature of cardiac cycle, unsteady flow is induced. In the modeled problem, arteries forming the bifurcation are taken symmetrical about the axis of the trunk. The blood considered as Newtonian fluid is flowing in the influence of a transverse static magnetic field. The expressions for flow velocity, volumetric flow rate (Q), wall shear stress (WSS) and wall shear stress gradient (WSSG) are derived and effects of various parameters on these hemodynamic indicators have been computed numerically and represented by graphs. The results show that the pattern of the velocity profiles and hemodynamic indices of the flowing blood alters in daughter vessel from that in the parent one.

Keywords- Bifurcating tube, Magnetohydrodynamic flow, Wall Shear Stress, Wall Shear Stress Gradient.

I. Introduction

The study of flow in a tube of circular cross-section has attracted the mathematician, engineers and the researchers for many years due to its importance in understanding the fluid mechanics in respect of blood flow. Womersley [1] has studied the pulsatile flow of viscous fluid due to given pressure gradient in a tube of circular cross-section. Uchida [2] investigated the analytic solution of the velocity profile for steady, incompressible flow in circular tube. Rao and Devanathan [3] found the result at low Reynolds number by considering the pulsatile flow through the circular tube of varying cross-section. Cen et al. [4] studied the oscillatory flow in circular pipe. They found a new solution for velocity and pressure gradient and resulted expression are found to be consistent with previous study. Cheng and Zhao [5] studied the reciprocating flows and associated heat transfer behavior in circular tubes. Steinman et al. [6] characterized the hemodynamic of moderately and severely stenosed carotid bifurcation. They concluded that the presence of a severe stenosis serves to increase the size and extent of the recirculation zones and introduces turbulence in the post-stenotic region. Sinnott et al. [7] investigated the pulsatile blood flow in a bifurcation artery using Grid-Free method. In this they used a real carotid bifurcation arterial geometry derived from MRI and gave the comparison between the pulsatile and steady flow. Sanyal et al. [8] developed a mathematical model for studying the characteristic of blood flow in a rigid inclined circular tube with periodic body acceleration under the influence of a uniform magnetic field and conclude that velocity increases with acceleration due to gravity, inclination and Womersley parameter and decreases with magnetic number. Deshpande et al. [9] simulated the subject specific blood flow in the human carotid artery bifurcation. They concluded that blood flow in the carotid bifurcation is associated with high wall shear stress and due to flow separation. The presence of even a mild stenosis may change the local flow considerably. They used the MRI and pulsed Doppler ultrasound techniques with CFD approach and found that this combined approach are superior than of medical imaging techniques. Blanco et al. [10] analyzed the various geometry of carotid bifurcation, three of them are based on a standard geometry with different degree of stenosis and fourth model was got from a patient-specie angiography using image segmentation and reconstruction techniques. The data obtained from their research was used to determine how geometry changes under the effect of various hemodynamic conditions. Chul et al. [11] studied the effects of periodic body acceleration and bifurcation angle in the stenosed artery bifurcation. They concluded that flow rate and wall shear stress increases with body acceleration and decrease with bifurcation angle. Also, high values of body acceleration generate back flow during the diastolic period, which increases flow variation OSI(oscillatory shear index)at the stenosis. Further they extended their work and in [12], they gave the results on turbulent blood flow in a stenosed artery bifurcation using a modified k- ϵ model. In this study they concluded that volumetric flow rate, blood velocity and amplitude of fluctuation increases as body acceleration increases. Also, a friction factor and the slope of the mean velocity profile varies according to the drag reduction in the non-Newtonian turbulent flow. Mansour et al. [13] performed the numerical investigation of unsteady, MHD free convection in an inclined square cavity and resulted that temperature increases with both of the magnetic field force and inclination angle and decreases with Rayleigh number.

Chakravarty and Sen [14] considered the blood flow through bifurcated stenosed artery to describe the dynamic response of heat and mass transfer. The blood velocity, the temperature and the concentration profiles

are obtained and represented by several graphs to illustrate the applicability of the model. Fan et al. [15] represented the Newtonian, the Casson and the hybrid fluid constitutive models for the blood flow of the human carotid bifurcation. They showed that for the axial velocity, secondary flow and wall shear stress, the Newtonian model and the hybrid model have the same pattern, while the Casson model had quite different results for these parameters. Wiwatanapataphee et al. [16] investigated the blood flow in the system of human coronary arteries considering the effects of branching of artery. They found that the profiles of velocity pressure and wall shear stress and concluded that due to the branching vessel of coronary arteries, the blood pressure decreases and wall shear stress increases. Suri and Suri [17] simulated the blood flow through a bifurcated tube under the influence of static magnetic field. They concluded that the within certain limits, the applied magnetic field reduces the strength of blockage at the apex of bifurcation and shear stress and alters the velocity of blood.

II. Formulation Of The Problem

The problem considered here is to study an unsteady pulsatile axially symmetric flow through asymmetrical branched vessel. The trunk is taken as circular vessel of radius R and of cross-sectional area A . Assuming branched diameter of the daughter branch is half of the diameter of the parent vessel then arteries with same cross sectional area A_1 and radius R_1 . Here, we considered the branch-to- trunk ratio = 1 ($R_1 = R$).

The angle formed between the two branches is 2θ . The axis of symmetry of both parent and daughter vessels are taken in the same plane. The axis of parent vessel is along z -axis, while axis of each of the daughter vessels are inclined at an angle θ with the z -axis. The wall of the vessel is taken as rigid wall, then the only non-zero velocity component be along the axis of the vessel with cylindrical co-ordinate system (r, θ, z) , where z -coincides with the axis of the parent vessel.

When an electrically conducting fluid like blood flow in a magnetic field, an electromagnetic force will be produced due to the interaction of current with magnetic field.

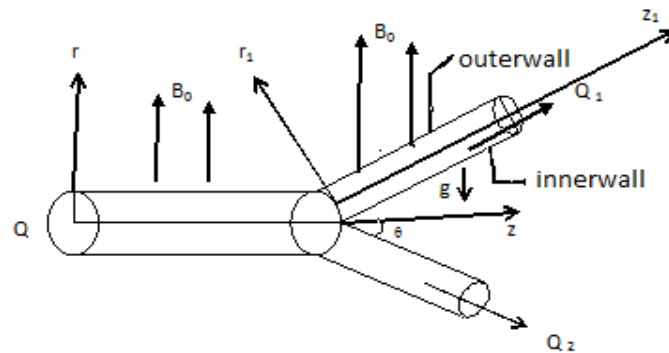


Fig.1: Physical model of the problem

The electromotive force is proportional to the speed of motion and the magnetic flux intensity B (Tashtoush and Magableh, [18]). The Maxwell's equations are

$$\text{div } \mathbf{B} = 0$$

$$\text{curl } \mathbf{B} = \mu_m \mathbf{J}$$

$$\text{curl } \mathbf{E} = -\frac{\partial \mathbf{B}}{\partial t}$$

Where \mathbf{E} is the electric field intensity, \mathbf{B} is the magnetic flux intensity μ_m is the electric permeability and \mathbf{J} is the current density. If σ is the electrical conductivity, Then generalized Ohm's law is

$$\mathbf{J} = \sigma(\mathbf{E} + \mathbf{V} \times \mathbf{B})$$

The induced electromagnetic force $F^{(em)}$ is defined as

$$F^{(em)} = \mathbf{J} \times \mathbf{B} = \sigma(\mathbf{E} + \mathbf{V} \times \mathbf{B}) \times \mathbf{B}$$

Following Cowling [19] that there is no applied or polarization voltage so that $\mathbf{E} = 0$. We assumed a magnetic field $\mathbf{B} = (B_0, 0, 0)$ with a constant transverse magnetic flux density B_0 of moderate strength so that induced magnetic field is negligible. The resultant force, the magnetohydrodynamic force is

$$F^{(em)} = \mathbf{J} \times \mathbf{B} = -\sigma B_0^2 w \hat{k}$$

Invoking these assumptions the governing equations of the motion of blood as Newtonian incompressible fluid with axisymmetric condition is given by

$$\frac{\partial u}{\partial t} = -\frac{1}{\rho} \frac{\partial p}{\partial z} + \nu \frac{1}{r} \frac{\partial}{\partial r} \left(r \frac{\partial u}{\partial r} \right) - \frac{\sigma B_0^2}{\rho} u \tag{1}$$

$$r=0: \quad \frac{\partial u}{\partial r} = 0$$

$$r=R_0: \quad u=0 \tag{2}$$

The arterial flow is governed by the periodic motion of heart in systolic and diastolic flow, therefore pressure gradient is of pulsating nature be in close proximity with actual physical condition. In view of this, taking pressure gradient in the following form :

$$\frac{\partial p}{\partial z} = \left(\frac{\partial p}{\partial z} \right)_s (1 + \gamma \cos(\omega t)) \tag{3}$$

Where $\left(\frac{\partial p}{\partial z} \right)_s$ is steady component of the pressure gradient and γ is the pressure fluctuation amplitude controlling parameter.

III. Method of solution

3.1 Calculation for velocity profiles of parent vessel

Taking $R_0, R_0^2 \nu, -\frac{R_0^2}{\mu} \left(\frac{\partial p}{\partial z} \right)_s$ and $\frac{1}{\rho} \left(\frac{\partial p}{\partial z} \right)_s$ as scaling parameter for length, time, velocity and acceleration respectively. Then non-dimensional form of equation (1) will be

$$\frac{\partial^2 u}{\partial r^2} + \frac{1}{r} \frac{\partial u}{\partial r} - H^2 u = \frac{\partial u}{\partial t} - (1 + \gamma \cos(\alpha^2 t)) \tag{4}$$

The corresponding boundary conditions are

$$r=0: \quad \frac{\partial u}{\partial r} = 0$$

$$r=1: \quad u=0$$

$$\text{where, } H^2 = \frac{R^2 \sigma B_0^2}{\mu} \quad \alpha^2 = \frac{R^2 \omega}{\nu} \tag{5}$$

For initial stage: The steady state flow equation is

$$\frac{\partial^2 u}{\partial r^2} + \frac{1}{r} \frac{\partial u}{\partial r} - H^2 u = -1 \tag{6}$$

The solution of this equation under B.C $r=1: u=0$ is

$$u(r) = \frac{1}{H^2} \left(1 - \frac{I_0(Hr)}{I_0(H)} \right) = F(r) \tag{7}$$

Applying the Laplace Transform defined by

$$L[u(r, t)] = \bar{u}(r, s) = \int_0^\infty u(r, t) \exp(-st) dt \tag{8}$$

From equation (4), We get

$$\frac{\partial^2 \bar{u}}{\partial r^2} + \frac{1}{r} \frac{\partial \bar{u}}{\partial r} - (H^2 + s) \bar{u} = -f(r) - \frac{1}{s} - \frac{\gamma s}{s^2 + \alpha^4} \tag{9}$$

Where $f(r) = u(r,0) = \frac{1}{H^2} \left(1 - \frac{I_0(Hr)}{I_0(H)} \right)$ is initial velocity in the parent vessel.

The corresponding boundary conditions are :

$$\begin{aligned} r=0 & : \quad \frac{\partial \bar{u}}{\partial r}(0, s) = 0 \\ r=1 & : \quad \bar{u}(1, s) = 0 \end{aligned} \tag{10}$$

The solution of equation (9) { using boundary condition $\bar{u}(1, s) = 0$ } in the Laplace space is obtained and given by

$$\bar{u}(r, s) = -\frac{I_0(\lambda r)}{I_0(\lambda)} \left(\frac{1}{s\lambda^2} + \frac{s\gamma}{\lambda^2(s^2 + \alpha^4)} + \frac{f(1)}{s} \right) + \frac{1}{s\lambda^2} + \frac{\gamma s}{\lambda^2(s^2 + \alpha^4)} + \frac{f(r)}{s} \tag{11}$$

where, $\lambda^2 = H^2 + s$

Applying inverse Laplace transform, we get

$$u(r, t) = \frac{1}{2\pi i} \int_{\gamma-i\infty}^{\gamma+i\infty} \exp \left\{ -\frac{I_0(\lambda r)}{I_0(\lambda)} \left(\frac{1}{s\lambda^2} + \frac{s\gamma}{\lambda^2(s^2 + \alpha^4)} + \frac{f(1)}{s} \right) + \frac{1}{s\lambda^2} + \frac{\gamma s}{\lambda^2(s^2 + \alpha^4)} + \frac{f(r)}{s} \right\} dr \tag{12}$$

Using residue theorem and the recurrence relation for Bessel's function, the expression for velocity distribution for parent vessel is given by

$$\begin{aligned} u_p(r, t) = & \frac{2}{H^2} \left[1 - \frac{I_0(Hr)}{I_0(H)} \right] + \left[1 - \frac{I_0(r\sqrt{H^2 + \alpha^2 i})}{I_0(\sqrt{H^2 + \alpha^2 i})} \right] \frac{\gamma \exp(it)}{2(H^2 + \alpha^2 i)} + \left[1 - \frac{I_0(r\sqrt{H^2 - \alpha^2 i})}{I_0(\sqrt{H^2 - \alpha^2 i})} \right] \frac{\gamma \exp(-it)}{2(H^2 - \alpha^2 i)} \\ & + 2 \sum_{n=1} \left[\frac{(\alpha_n^2 + H^2)\gamma}{\alpha_n(\alpha^4 + \alpha_n^4 + H^4 + 2\alpha_n^2 H^2)} + \frac{1}{\alpha_n(\alpha_n^2 + H^2)} \right] \frac{J_0(\alpha_n r)}{J_1(\alpha_n)} \exp \left(-\frac{(\alpha_n^2 + H^2)t}{\alpha^2} \right) \end{aligned} \tag{13}$$

3.2 Calculation for Hemodynamic indicator Volumetric Flow Rate (Q_p)

The Volumetric flow rate through the parent vessel is given by

$$\begin{aligned} Q_p = & 2\pi \int_0^1 r u dr \\ = & \frac{1}{H^2} \left[1 - \frac{2I_1(H)}{I_0(H)H} \right] + \left[\frac{1}{2} - \frac{I_1(\sqrt{H^2 + \alpha^2 i})}{(\sqrt{H^2 + \alpha^2 i})I_0(\sqrt{H^2 + \alpha^2 i})} \right] \frac{\gamma \exp(it)}{2(H^2 + \alpha^2 i)} + \\ & \left[\frac{1}{2} - \frac{I_1(\sqrt{H^2 - \alpha^2 i})}{\sqrt{H^2 - \alpha^2 i}I_0(\sqrt{H^2 - \alpha^2 i})} \right] \frac{\gamma \exp(-it)}{2(H^2 - \alpha^2 i)} \\ & + 2 \sum_{n=1} \left[\frac{(\alpha_n^2 + H^2)\gamma}{\alpha_n^2(\alpha^4 + \alpha_n^4 + H^4 + 2\alpha_n^2 H^2)} + \frac{1}{\alpha_n^2(\alpha_n^2 + H^2)} \right] \exp \left(-\frac{(\alpha_n^2 + H^2)t}{\alpha^2} \right) \end{aligned} \tag{14}$$

3.3 Calculation for Hemodynamic indicator Wall Shear Stress (WSS_p):

The Wall Shear Stress at the surface of the parent vessel is given by

$$\begin{aligned}
 \text{WSS}_p &= - \left[\frac{\partial u}{\partial r} \right]_{r=1} \\
 &= \frac{2}{H} \left[\frac{I_1(H)}{I_0(H)} \right] + \left[\frac{I_1(\sqrt{H^2 + \alpha^2 i})}{I_0(\sqrt{H^2 + \alpha^2 i})} \right] \frac{\gamma \exp(it)}{2\sqrt{H^2 + \alpha^2 i}} + \left[\frac{I_1(\sqrt{H^2 - \alpha^2 i})}{I_0(\sqrt{H^2 - \alpha^2 i})} \right] \frac{\gamma \exp(-it)}{2\sqrt{H^2 - \alpha^2 i}} \\
 &+ 2 \sum_{n=1} \left[\frac{(\alpha_n^2 + H^2) \gamma}{(\alpha^4 + \alpha_n^4 + H^4 + 2\alpha_n^2 H^2)} + \frac{1}{(\alpha_n^2 + H^2)} \right] \exp \left(- \frac{(\alpha_n^2 + H^2)t}{\alpha^2} \right) \quad (15)
 \end{aligned}$$

3.4 Calculation for Hemodynamic indicator Wall Shear Stress (WSSG_p) :

The Wall Shear Stress Gradient through the parent vessel is given by

$$\begin{aligned}
 \text{WSSG}_p &= \frac{\partial \tau}{\partial t} \\
 &= \left[\frac{I_1(\sqrt{H^2 + \alpha^2 i})}{I_0(\sqrt{H^2 + \alpha^2 i})} \right] \frac{\gamma i \exp(it)}{2\sqrt{H^2 + \alpha^2 i}} - \left[\frac{I_1(\sqrt{H^2 - \alpha^2 i})}{I_0(\sqrt{H^2 - \alpha^2 i})} \right] \frac{\gamma i \exp(-it)}{2\sqrt{H^2 - \alpha^2 i}} \\
 &+ 2 \sum_{n=1} \left[\frac{(\alpha_n^2 + H^2) \gamma}{(\alpha^4 + \alpha_n^4 + H^4 + 2\alpha_n^2 H^2)} + \frac{1}{(\alpha_n^2 + H^2)} \right] \exp \left(- \frac{(\alpha_n^2 + H^2)t}{\alpha^2} \right) \left(- \frac{(\alpha_n^2 + H^2)}{\alpha^2} \right) \quad (16)
 \end{aligned}$$

3.5 Calculation for velocity profiles of daughter vessel:

Let orthogonal axis r_1 and z_1 are lying in the plane of the geometry and inclined with r and z axis at an angle θ , then non-dimensional form of the equation for flow in daughter vessel is given by

$$\frac{\partial^2 u_1}{\partial r_1^2} + \frac{1}{r_1} \frac{\partial u_1}{\partial r_1} - H^2 \cos^2 \theta u_1 = \alpha^2 \frac{\partial u_1}{\partial t} - (1 + \gamma \cos(\alpha^2 t) + g \sin \theta) \quad (17)$$

The corresponding boundary conditions are

$$\begin{aligned}
 r_1 = 0 & : \quad \frac{\partial u_1}{\partial r_1} = 0 \\
 r_1 = \frac{R_1}{R} & : \quad u_1 = 0 \quad (18)
 \end{aligned}$$

The fundamental fact that the rate of flow into and out of the system must be equal i.e

$$Q = 2Q_1 \quad (19)$$

with the help of this condition, the flow velocity at the entrance of the daughter branch can be obtained and gives initial condition for flow in branch region, i.e

$$2 \int_0^{\frac{R_1}{R}} r_1 u_1(r, t) dr_1 = \int_0^1 r u(r, t) dr \quad (20)$$

The solution of equation (17) (Using the linear transformation: $r_1 = r \cos \theta$) is given by

$$\begin{aligned}
 u_d(r,t) = & \frac{(1 + g \sin \phi)}{H^2 \cos^2 \phi} \left[1 - \frac{I_0(H \cos^2 \phi r)}{I_0\left(H \cos \phi \frac{R_1}{R}\right)} \right] + \left[1 - \frac{I_0\left((r \cos \phi)\sqrt{H^2 \cos^2 \phi + \alpha^2 i}\right)}{I_0\left(\sqrt{H^2 \cos^2 \phi + \alpha^2 i} \frac{R_1}{R}\right)} \right] \frac{\gamma \exp(it)}{2(H^2 \cos^2 \phi + \alpha^2 i)} \\
 & + \left[1 - \frac{I_0\left((r \cos \phi)\sqrt{H^2 \cos^2 \phi - \alpha^2 i}\right)}{I_0\left(\sqrt{H^2 \cos^2 \phi - \alpha^2 i} \frac{R_1}{R}\right)} \right] \frac{\gamma \exp(-it)}{2(H^2 \cos^2 \phi - \alpha^2 i)} \\
 & + 2 \sum_{n=1}^{\infty} \left[\frac{\left(\alpha_n^2 \frac{R^2}{R_1^2} + H^2 \cos^2 \phi\right) \gamma}{\alpha_n \left(\alpha^4 - \alpha_n^2 \frac{R^2}{R_1^2} - H^2 \cos^2 \phi\right)} + \frac{(1 + g \sin \phi)}{\alpha_n \left(\alpha_n^2 \frac{R^2}{R_1^2} + H^2 \cos^2 \phi\right)} \right. \\
 & \left. - \frac{\alpha_n \left(\frac{R}{R_1}\right)^2 f\left(\frac{R_1}{R}\right)}{\left(\alpha_n^2 \left(\frac{R}{R_1}\right)^2 + H^2 \cos^2 \phi\right)} \right] \frac{J_0\left(\alpha_n \frac{R}{R_1} r \cos \phi\right)}{J_1(\alpha_n)} \exp\left(-\frac{\left(\alpha_n^2 \frac{R^2}{R_1^2} + H^2 \cos^2 \phi\right) t}{\alpha^2}\right) \\
 & + f_1(r \cos \phi) - f_1\left(\frac{R_1}{R}\right) \frac{I_0(H \cos^2 \phi r)}{I_0\left(H \cos \phi \frac{R_1}{R}\right)}
 \end{aligned} \tag{21}$$

3.6 Calculation for Hemodynamic indicator Wall Shear Stress (WSS_d) :

The Wall Shear Stress at the surface of daughter branch is given by

$$\begin{aligned}
 WSS_d = & - \left[\frac{\partial u_1}{\partial r_1} \right]_{r_1=1} \\
 = & \frac{2(1 + g \sin \phi)}{H} \left[\frac{I_1(H \cos^2 \phi)}{I_0(H \cos \phi)} \right] + \left[\frac{I_1(\sqrt{H^2 \cos^2 \phi + \alpha^2 i})}{I_0(\sqrt{H^2 \cos^2 \phi + \alpha^2 i})} \right] \frac{\gamma \exp(it)}{2\sqrt{H^2 \cos^2 \phi + \alpha^2 i}} \\
 & + \left[\frac{I_1(\sqrt{H^2 \cos^2 \phi - \alpha^2 i})}{I_0(\sqrt{H^2 \cos^2 \phi - \alpha^2 i})} \right] \frac{\gamma \exp(-it)}{2\sqrt{H^2 \cos^2 \phi - \alpha^2 i}} \\
 & + 2 \sum_{n=1}^{\infty} \left[\frac{\left(\alpha_n^2 + H^2 \cos^2 \phi\right) \gamma}{\left(\alpha^4 + \alpha_n^4 + H^4 \cos^4 \phi + 2\alpha_n^2 H^2 \cos^2 \phi\right)} + \frac{1}{\left(\alpha_n^2 + H^2 \cos^2 \phi\right)} \right] \\
 & \exp\left(-\frac{\left(\alpha_n^2 + H^2 \cos^2 \phi\right) t}{\alpha^2}\right) \frac{J_1(\alpha_n \cos \phi)}{J_1(\alpha_n)} \cos \phi
 \end{aligned} \tag{22}$$

3.7 Calculation for Hemodynamic incator Wall Shear Stress Gradient (WSSG_d)

The Wall Shear Stress Gradient for daughter branch

$$\begin{aligned}
 WSSG_d &= \frac{\partial \tau}{\partial t} \\
 &= \left[\frac{I_1(\sqrt{H^2 \cos^2 \theta + \alpha^2} i)}{I_0(\sqrt{H^2 \cos^2 \theta + \alpha^2} i)} \right] \frac{\gamma i \exp(it)}{2\sqrt{H^2 \cos^2 \theta + \alpha^2} i} \\
 &\quad - \left[\frac{I_1(\sqrt{H^2 \cos^2 \theta - \alpha^2} i)}{I_0(\sqrt{H^2 \cos^2 \theta - \alpha^2} i)} \right] \frac{\gamma i \exp(-it)}{2\sqrt{H^2 \cos^2 \theta - \alpha^2} i} \\
 &\quad + 2 \sum_{n=1}^{\infty} \left[\frac{(\alpha_n^2 + H^2 \cos^2 \theta) \gamma}{(\alpha^4 + \alpha_n^4 + H^4 \cos^4 \theta + 2\alpha_n^2 H^2 \cos^2 \theta)} + \frac{1}{(\alpha_n^2 + H^2 \cos^2 \theta)} \right] \\
 &\quad \exp\left(-\frac{(\alpha_n^2 + H^2 \cos^2 \theta)t}{\alpha^2}\right) \left(-\frac{(\alpha_n^2 + H^2 \cos^2 \theta)}{\alpha^2}\right) \frac{J_1(\alpha_n \cos \theta)}{J_1(\alpha_n)} \cos \theta
 \end{aligned} \tag{23}$$

IV. Results And Discussion

The expression of axial velocity , volumetric flow rate, wall shear stress and wall shear stress gradient are obtained and computed data are plotted for different values of Hartmann number(H) ,Womersley number (α) and inclination angle(θ) for both parents vessel and daughter vessel .

The profiles of axial velocity u_p versus radial co-ordinate for various physical parameters are shown in Figs. 2 and 3 for the parents vessel. Fig. 2, depicts that with the increase of Hartmann number the flowing fluid is slowed down in axial direction. Besides, deceleration in the flow with increase of Hartmann number the axial velocity profile ceases to remain parabolic and becomes flatten at the centerline region. For H=5 the velocity profile is almost flat at the centerline region. Fig. 3 demonstrates that the axial flow u_p velocity increases on increasing Womersley number, i.e. flow velocity will be augmented by raising the oscillation in the flow. Figs. 4 and 5 demonstrates that volumetric flow rate of the fluid decreases with Hartmann number and increases with Womersley number. Figs. 6 and 7 show the effect of magnetic field and Womersley number on wall shear stress for parents vessel. WSS_p increases with the increase of magnetic field which is in good agreement with earlier investigation. Figs. 8 and 9 demonstrates the effect of magnetic field and Womersley number on wall shear stress gradient (WSSG_p) for parents vessel. $WSSG_p$ increases with the increase of magnetic field for $\alpha \geq 2$. Also from Fig. 9, it is seen that $WSSG_p$ decreases with Womersley number.

Figs. 10 and 11 show that axial velocity u_d is more pronounced in daughter vessel for same values of parameters H and α . Figure 12 depicts that axial velocity u_d increases on increasing inclination θ. Also from Fig. 13, it is seen that WSS_d for daughter vessel reduces its value that of parents vessel. Fig. 7 depicts that WSS_p increases with the increase of Womersley number. WSS_d also follow the same pattern with a small decrease in value as shown in Fig. 14. Figs. 15 and 16 depict the variation of WSS_d versus inclination and shows that WSS_d increases with Hartmann number and Womersley number. Fig. 17 depicts that $WSSG_d$ increases for $\alpha \geq 2$ with the increase of Hartmann number having values somewhat greater than parents vessel and $WSSG_d$ decreases with the increase of Womersley number as seen from Fig. 18. Here is also the variation of sign in the region $1.5 \leq \alpha \leq 2$ for both parents and daughter vessels. Figs. 19 and 20 shows the variation of $WSSG_d$ versus inclination θ, $WSSG_d$ increases with Hartmann number $H \leq 3$ and then a decrease is observe for H=4 and H=5 and there is a sharp decrease with increase of Womersley number as in Fig. 20.

V. Conclusions

This study represents the pulsatile blood flow through bifurcated artery under the influence of transverse magnetic field. Here we calculated effect of magnetic field on various fluid parameters like blood velocity, volumetric flow rate, wall shear stress, wall shear stress gradient numerically. Since the technical tools for the understanding of arterial diseases like MRI(Magnetic Resonance Imaging) can be costly and provide only a little knowledge about the flow, in this case , the present study promotes the researchers to have an idea about the conditions and flow pattern to be modified for the diagnose of arterial diseases.

References

- [1]. J. R. Womersley, Method for calculation of velocity, rate of flow and viscous drag when pressure gradient is know, *Physiol*, 127, 1955, 553-563.
- [2]. S.Uchida, The pulsating viscous flow superposed on the steady laminar motion of incompressible fluid in a circular pipe, *ZAMP*, 7, 1956, 403-422.
- [3]. A.R. Rao, and R. Devanathan, Pulsatile flow in tubes of varying cross- section, *ZAMP*, 24, 1973, 203-213.
- [4]. R.J. Cen, and B.S. Liu, Developing oscillatory flow in a circular pipe: A new solution, *Biomechanical Engineering*, 109, 1987, 340-345.
- [5]. T. S. Zhao and P. Cheng, The friction coefficient of laminar oscillatory flow in a circular pipe, *Heat Fluid Flow*, 17, 1996, 167-172.
- [6]. D. Steinman, A. Poepping, L. Tamie, M. Tambasco, R. N. Rankin, and D. W. Holdsworth, Flow patterns at the stenosed carotid bifurcation: effect of concentric versus eccentric stenosis, *Annals of Biomedical Engineering*, 28, 2000, 415-423.
- [7]. M. Sinnott, P.W. Cleary, and M. Prakesh, An investigation of pulsatile blood flow in a bifurcation artery using a grid – free method, Fifth International conference on CFD in the process industries, CSIRO, Melbourne (Australia), December, 2006, 13-15.
- [8]. D.C. Sanyal, K. Das, and S. Debnath, Effect of magnetic field on pulsatile blood flow through an inclined circular tube with periodic body acceleration, *Physical Sciences*, 11, 2007, 43-56.
- [9]. M.D. Deshpande, V. Ballali, S.R. Shankapali, M.D. Vinay, Prabhu, and M.G. Srinath, Subject-specific blood flow simulation in the human carotid artery bifurcation, *Current Sciences*, 97(9), 2009, 1303-1312.
- [10]. P. J. Blanco, I. Larrabide, S. A Urquiza, and R. A Feijoo, Sensitivity of blood flow in the stenosed carotid bifurcation, International Conferene on Comp. Bioengineering, Lisbon, 2005, 14-16.
- [11]. K.C. Ro, and H .S. Ryou, Numerical study of the effects of periodic body acceleration (PGZ) and bifurcation angle in the stenosed artery bifurcation, *Korea-Australia Rheology*, 21(3), 2009, 175-183.
- [12]. K.C. Ro, and H. S. Ryou, Numerical study on turbulent blood flow in a stenosed artery bifurcation under periodic body acceleration using a modified k-ε model, *Korea-Australia Rheology*, 22(2), 2010, 129-139.
- [13]. M.A. Mansour, A.J. Chamkha, R.A. Mohamed, S.E. Ahmed, MHD natural convection in an inclined cavity filled with a fluid saturated porous medium with heat source in the solid phase, *Non-linear Analysis: Modelling and Control*, 15(1), 2010, 55-70.
- [14]. S. Chakravarty and s. Sen, Dynamic response of heat and mass transfer in blood flow through stenosed bifurcated arteries, *Korea-Australia Rheology Journal*, 17(2), 2005, 47-62.
- [15]. Y. Fan, W. Jiang, Y. Zou, J. Li, J. Chen and X. Deng, Numerical simulation of pulsatile non-Newtonian flow in the carotid artery bifurcation, *Acta Mechanica Sinica*, 25(2), 2009, 249-255.
- [16]. B. Wiwatanapataphee, Y.H. Wu, T. Siriapish and B. Nuntadilok, Effect of branchings on blood flow in the system of human coronary arteries, *Mathematical Biosciences and Engineering*, 9(1), 2012, 199-214.
- [17]. P.K. Suri and P. R. Suri, Effect of static magnetic field on blood flow in a branch, *Indian J. Pure and Appl. Math.*, 12(7), 191, 907-918.
- [18]. B. Tashtoush and A. Magableh, Magnetic field effect on heat transfer and fluid flow characteristics of blood flow in multi-stenotic arteries, *Heat and Mass Transfer*, 44(3), 2008, 297-304.
- [19]. T. G. Cowling, *Magnetohydrodynamics* (Interscience Publishers, New York, 1957).

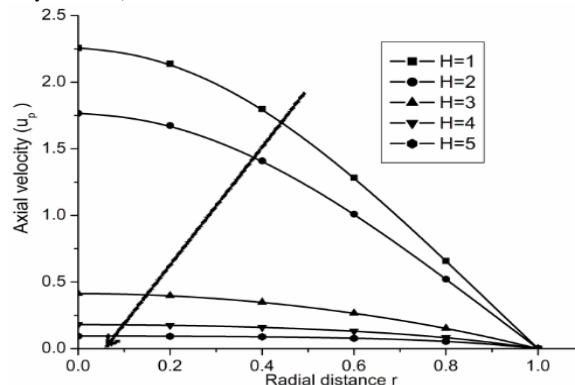


Fig. 2: Variation of axial velocity with Hartmann number for parent vessel at $\alpha=1.83$

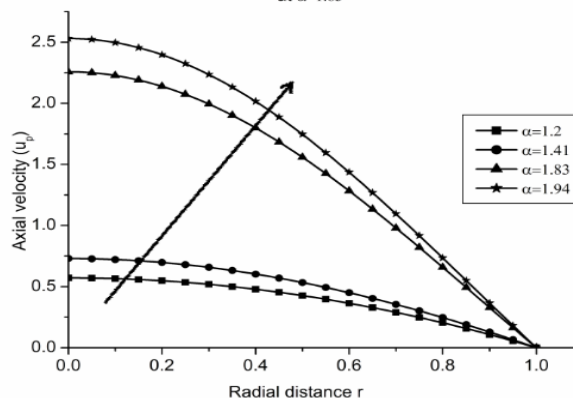


Fig. 3: Variation of Axial velocity with Womersley number for parent vessel at $H=1$

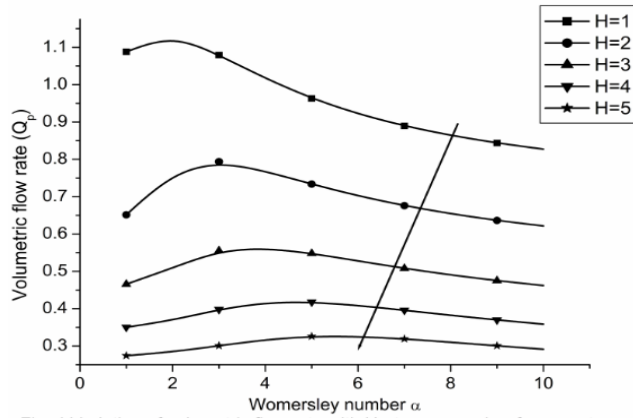


Fig. 4:Variation of volumetric flow rate with Hartmann number for parent vessel

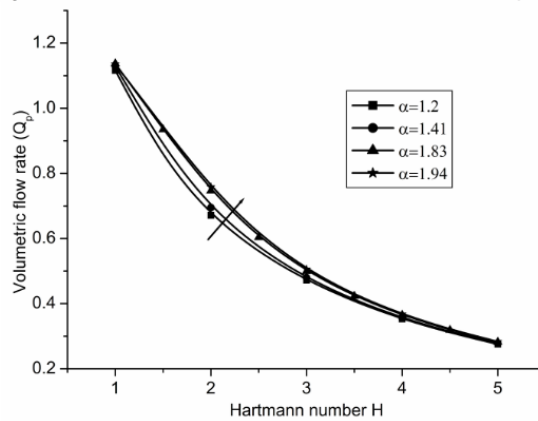


Fig. 5:Variation of volumetric flow rate with Womersley number for parent vessel

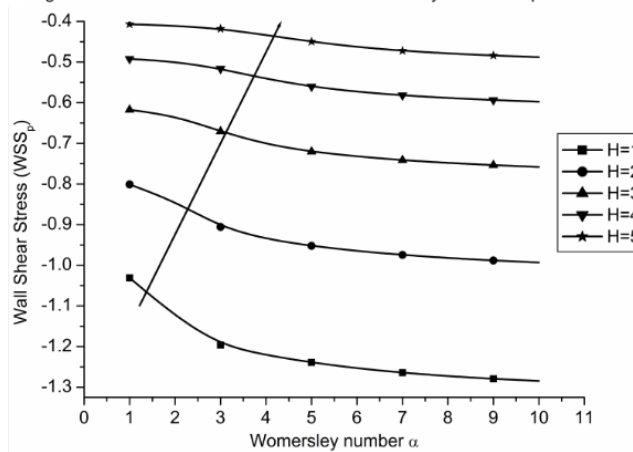


Fig. 6: Variation of wall shear stress with Hartmann number for parent vessel

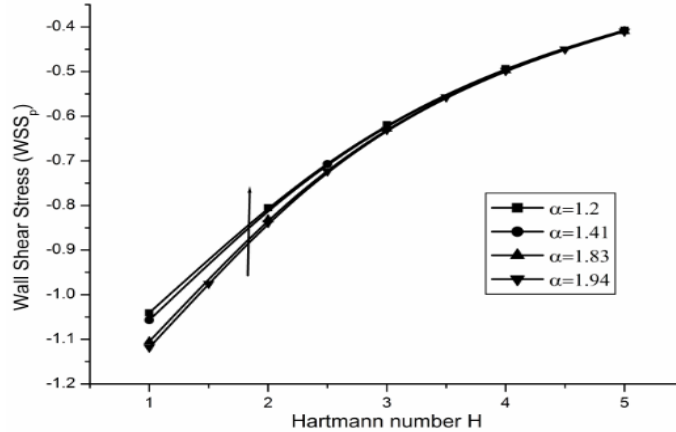


Fig. 7:Variation of wall shear stress with Womersley number for parent vessel

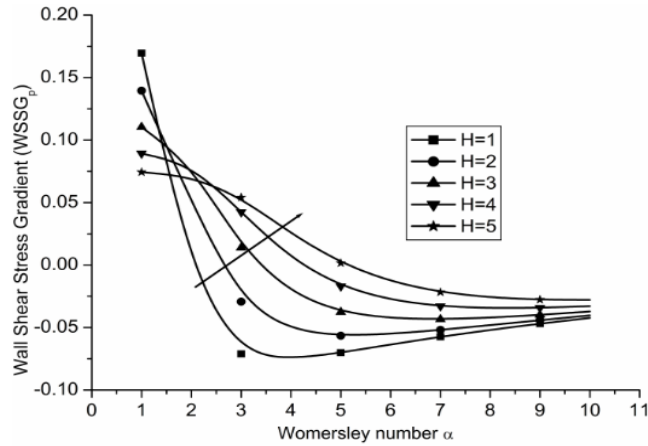


Fig. 8: Variation of wall shear stress gradient with Hartmann number for parent vessel

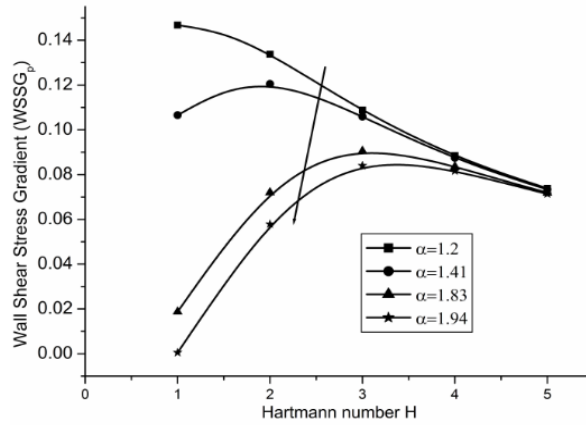


Fig. 9: Variation of wall shear stress gradient with Womersley number for parent vessel

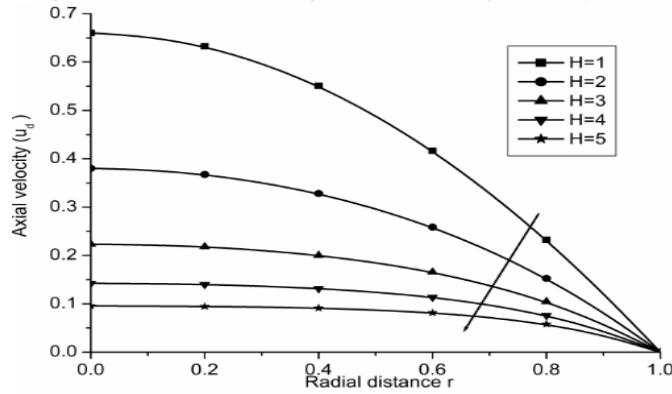


Fig. 10: Variation of axial velocity with Hartmann number for daughter vessel at $\alpha=1.2, g=9.8, \phi=\pi/12$

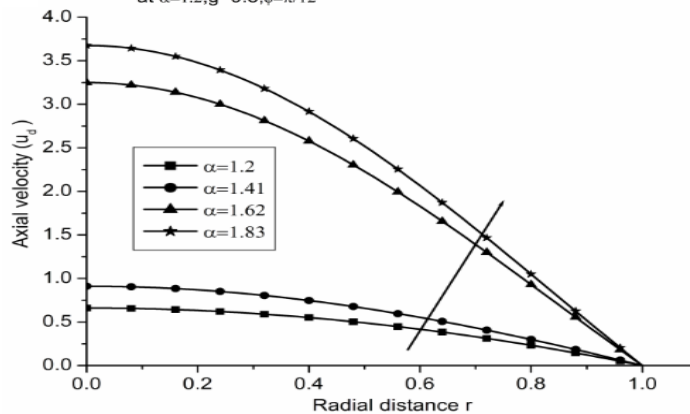


Fig. 11: Variation of axial velocity with Womersley number for daughter vessel at $H=1, g=9.8, \phi=\pi/12$

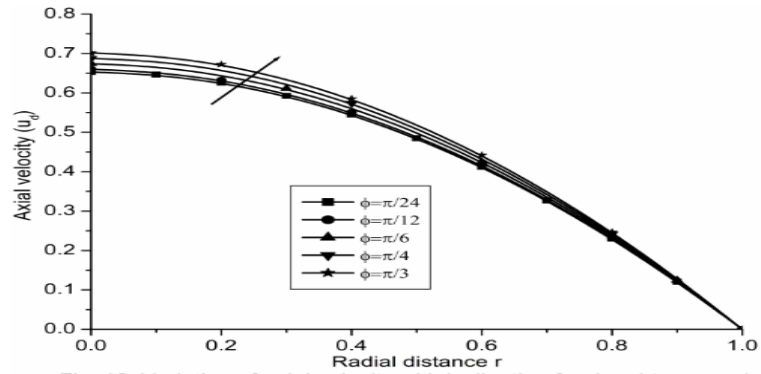


Fig. 12: Variation of axial velocity with inclination for daughter vessel at $H=1, g=9.8, \alpha=1.2$

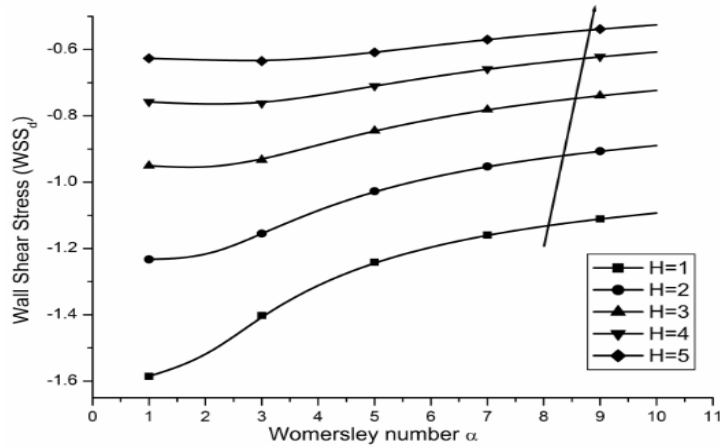


Fig. 13: Variation of wall shear stress with Hartmann number for daughter vessel at $g=9.8, \phi=\pi/12$

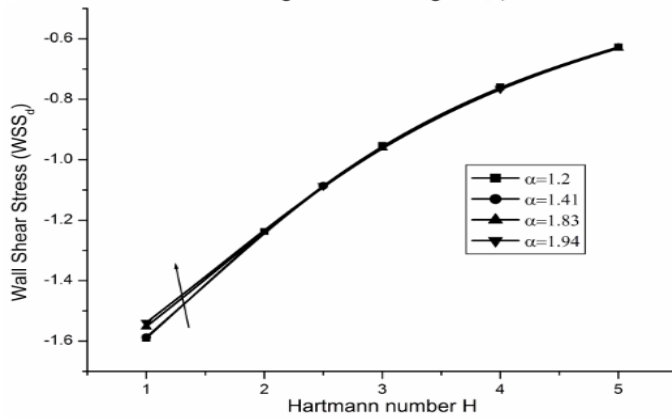


Fig. 14: Variation of wall shear stress with Womersley number for daughter vessel at $g=9.8, \phi=\pi/12$

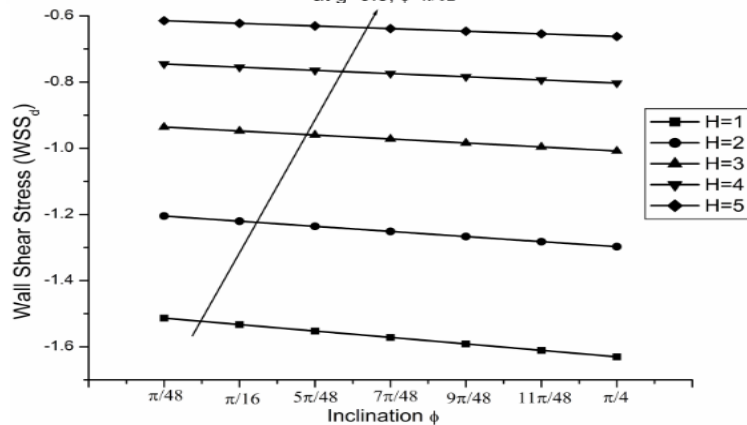


Fig. 15: Variation of wall shear stress with Hartmann number for daughter vessel at $g=9.8, \alpha=1.2$

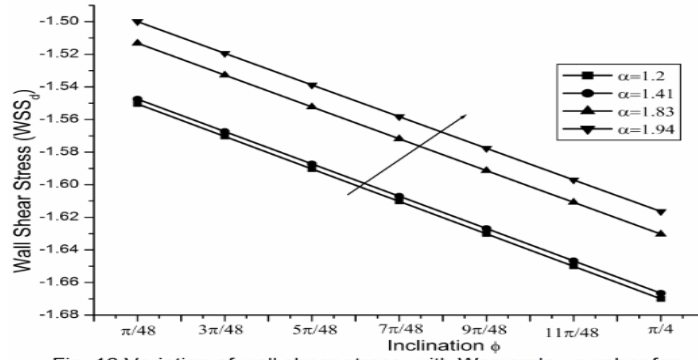


Fig. 16: Variation of wall shear stress with Womersley number for daughter vessel at $g=9.8, H=1$

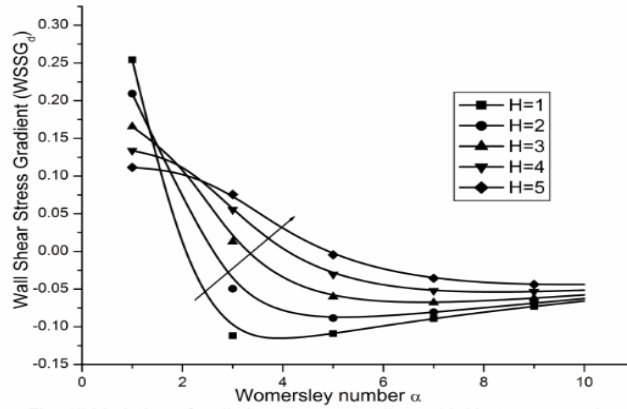


Fig. 17: Variation of wall shear stress gradient with Hartmann number for daughter vessel at $g=9.8, \phi=\pi/12$

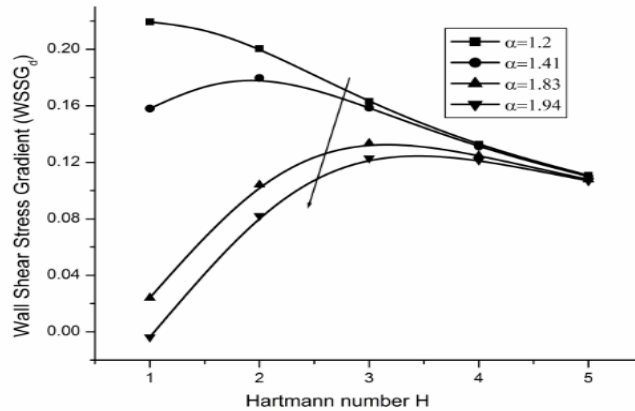


Fig. 18: Variation of wall shear stress gradient with Womersley number for daughter vessel at $g=9.8, \phi=\pi/12$

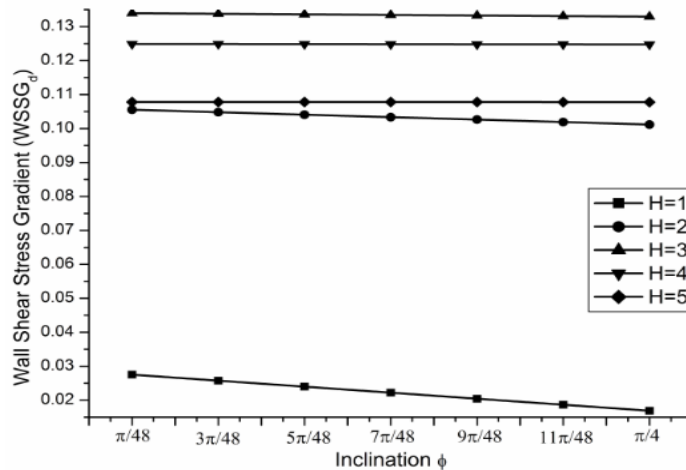


Fig. 19: Variation of wall shear stress gradient with Hartmann number for daughter vessel at $g=9.8, \alpha=1.2$

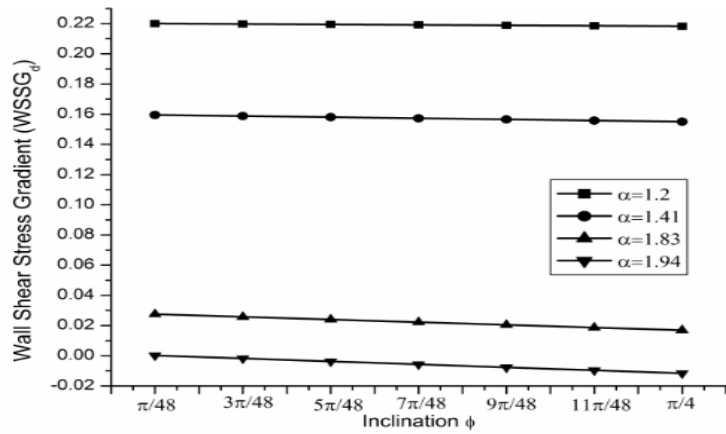


Fig. 20: Variation of wall shear stress gradient with Womersley number for daughter vessel at $g=9.8$, $H=1$